Receivers for the up-link of multiuser MIMO systems with Spatial Modulation

José Luis Calpa Juajinoy, João Alfredo Cal-Braz and Raimundo Sampaio-Neto

Abstract— **This paper presents the results obtained from the conjunction of two techniques proposed for use in modern communication systems: Spatial Modulation (SM) and decoupled signal detection. Theoretical fundamentals of Spatial Modulation signal detection are covered, in addition to signal decoupling techniques that enable the separation at the base station of signals transmitted from different users, aiming at the simplification and utilization of detection procedures best suited to each user in the network. Performance analyses, in terms of bit error rate, and computational complexity, in terms of the average number of flops per detected symbol vector are carried out for the different associations of decoupling techniques and SM detectors.**

Keywords— **MIMO systems, Up-link, Spatial Modulation, Decoupling signal detection.**

I. Introduction

The use of Spatial Modulation in MIMO systems [1], [2] allows the reduction of the number of RF chains used in the signal transmission, with consequent reduction of cost and energy spent by the transmitters. This work is focused in one alternative to simplify the received signal processing in the base station of systems with Generalized Spatial Modulation [3], combining decoupling techniques with efficient techniques for the signal detection in such systems. The presented proposal in this article is aligned with the future wireless communications developments, because presents methods to process the multiple users that demand connectivity of the BS, enabling the use of decoupling and detection methods best suited to their specific performance requirements. In addition, it provides means to reduce the costs of transmit system devices, by the reduction of the number of RF chains caused by the use of the Spatial Modulation.

II. SM-MU System

A. Scenario description

The diagram depicted in Figure 1 presents a MIMO SM-MU system, in which users communicate to a base station(BS). Users with similar service requirements are grouped, so equal treatment will be applied to them at the receiver, totaling N user classes. The n-th class, C_n, is composed by D_n users and each of them transmits data using spatial modulation. Consider that each user in this class has N_{T_n} transmit antennas, and that at each transmission timeslot only N_{A_n} antennas are actived, and through them independent QAM symbols are transmitted. The choice of the active antennas are commanded by the data to be transmitted by this user, as defined in the mapping table. For instance, consider a user of class n, equipped with $N_{T_n} = 4$ and $N_{A_n} = 2$. Under this configuration, the number of permissible antenna configurations N_c equals the power of two immediately lower than $\binom{N_{T_n}}{N_{A_n}}$, or equal to 4, in this example. So, input binary data are mapped into antenna combinations, as exemplified in the antenna combination mapping table (ACMT), presented in Table 1. As a result, the number of bits transmitted per timeslot equals the sum of the bits related to the antenna combination and the bits associated to the QAM symbols transmitted by the active antennas. Equal number of transmit antennas and ACMT will be admitted for users under the same class, even though the presented mathematical expressions are easily extended to the general case and the proposed strategies are applicable to the general case.

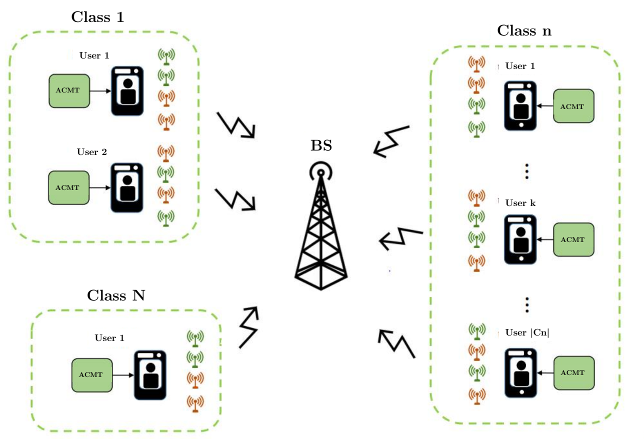

Fig. 1. SM-MU MIMO scenario.

B. Signal model - System up-link

Let the cardinality of n-th class $|C_n| = D_n$, the number of antennas $M_{T_n} = D_n N_{T_n}$, the number of active antennas $M_{A_n} = D_n N_{A_n}$ and the total number of transmit antennas of the system $M_T = \sum_{n=1}^{N} M_{T_n}$. The symbol vector transmitted in the active antennas by the users of the n-th class, $\mathbf{b}_n$, concatenates the symbol

José Luis Calpa Juajinoy and Raimundo Sampaio-Neto, Center for Telecommunications Research - CETUC, Pontifical Catholic University of Rio de Janeiro, Rio de Janeiro-RJ, Brasil, E-mails: joselocalpa14@cetuc.puc-rio.br, raimundo@cetuc.puc-rio.br and João Cal-Braz. National Institute of Metrology, Quality and Technology - INMETRO, E-mail: jabraz@inmetro.gov.br

Input Bits	Antenna 1	Antenna 2	Antenna 3	Antenna 4
00	1	1	0	0
01	1	0	1	0
10	0	1	0	1
11	0	0	1	1

TABLE I

EXAMPLE OF A MAPPING TABLE ACMT FOR $N_{T_n} = 4$ AND $N_{A_n} = 2$. ENTRIES 1 AND 0 REPRESENT ACTIVE AND NON-ACTIVE ANTENNAS, RESPECTIVELY.

vectors of the each user of the class, $\mathbf{b}_{n,i}$ producing $\mathbf{b}_n = [\mathbf{b}_{n,1}^T \;\; \mathbf{b}_{n,2}^T \;\; \ldots \;\; \mathbf{b}_{n,D_n}^T]^T$, with dimension $M_{A_n} \times 1$. The SM-MU data vector transmitted by the users in class n are allocated in the vector $\mathbf{s}_n = [\mathbf{s}_{n,1}^T \;\; \mathbf{s}_{n,2}^T \;\; \ldots \;\; \mathbf{s}_{n,D_n}^T]^T$, with dimension $M_{T_n} \times 1$, which contains zeros in the entries related to non active antennas and the symbols contained in $\mathbf{b}_n$, drawn from a digital constellation represented by the set $\mathbb{B}$, in the entries that correspond to active antennas. Also, consider that, in class n, the first user employs the p_1-th ACMT antenna combination, the second user uses the p_2-th antennas combination and so forth. The matrix that positions the elements of $\mathbf{b}_{n,k}$ in the non-zero entries of $\mathbf{s}_{n,k}$ is given by the matrix $\mathbf{P}_{p_k}^n$. The vectors $\mathbf{b}_n$ and $\mathbf{s}_n$ are related by $\mathcal{P}^{(n)}$, as given by:

$$\mathbf{s}_n = \mathcal{P}^{(n)} \mathbf{b}_n \tag{1}$$

where $\mathcal{P}^{(n)} = [\mathbf{P}_{p_1} \;\; \mathbf{P}_{p_2} \;\; \ldots \;\; \mathbf{P}_{p_{D_n}}]$.

The elements of $\mathbf{s}_n$ belong to the set $\mathcal{S}_n$:

$$\mathcal{S}_n = \{\mathcal{P}^{(n)} \mathbf{b}_n \; | p_1, p_2, \ldots, p_{|c_n|} \in 1, 2, \ldots, N_{c_n}, \mathbf{b}_n \in \mathbb{B}^{M_{A_n}}\} \tag{2}$$

The signal that traverses the multiuser MIMO channel arrives at the BS. It is related to the signal transmitted by the $\sum_{n=1}^{N} |C_n|$ users by:

$$\mathbf{y} = \sum_{n=1}^{N} \sum_{k=1}^{|C_n|} \mathbf{H}_{n,k} \mathbf{s}_{n,k} + \mathbf{n}, \tag{3}$$

where $\mathbf{H}_{n,k}$ is the $N_r \times N_{t_n}$ channel matrix that links the N_{t_n} antennas of the k-th user of the n-th class and the N_r receive antennas at the BS. The additive Gaussian noise is zero mean and covariance matrix equal to $\mathbf{K}_n = \sigma_n^2 \mathbf{I}_{N_r}$. The expression in (3) can be rewritten as:

$$\mathbf{y} = \sum_{n=1}^{N} \mathbf{H}_n \mathbf{s}_n + \mathbf{n}, \tag{4}$$

where $\mathbf{H}_n = [\mathbf{H}_{n,1} \;\; \mathbf{H}_{n,2} \ldots \mathbf{H}_{n,|C_n|}]$ and $\mathbf{s}_n = [\mathbf{s}_{n,1}^T \;\; \mathbf{s}_{n,2}^T \ldots \mathbf{s}_{n,|C_n|}^T]^T$ represent the channel matrix $N_r \times M_{t_n}$ that links the users of class n with BS and the symbol vector transmitted by all users in class n, respectively. Finally, the received vector is expressed by:

$$\mathbf{y} = \mathbf{H}\mathbf{s} + \mathbf{n}, \tag{5}$$

where $\mathbf{H} = [\mathbf{H}_1 \;\; \mathbf{H}_2 \ldots \mathbf{H}_N]$ with dimension $N_r \times M_t$ and $\mathbf{s} = [\mathbf{s}_1^T \;\; \mathbf{s}_2^T \ldots \mathbf{s}_N^T]^T$ $M_t \times 1$. Considering that the user symbol vectors, $\mathbf{s}_{n,k}$, transmit MIMO-GSM symbols with energy E_{s_n}, then $\mathbb{E}[\mathbf{s}_{n,k}^H \mathbf{s}_{n,k}] = N_{A_n} E_{s_n}$. Then, for the data vectors with all users, $\mathbf{s}$, $\mathbb{E}[\mathbf{s}^H \mathbf{s}] = D_1 N_{A_1} E_{s_1} + D_2 N_{A_2} E_{s_2} + \cdots + D_N N_{A_N} E_{s_N}$. For the sake of simplicity of notation and the analyses that follows, admit that users emit symbols with the same average energy, E_s, so $\mathbb{E}[\mathbf{s}^H \mathbf{s}] = E_s \sum_{n=1}^{N} M_{A_n}$. The signal-to-noise ratio (SNR) per received antenna at the BS is defined as $SNR = 10 \log_{10}(M_{A_n} E_s / \sigma_n^2)$. The perfect knowledge of the channel $\mathbf{H}$ at the BS is also assumed.

III. RECEIVERS

In this section, receivers for SM-MU systems are proposed. These receivers are comprised of decouplers, that remove the interference of the other users over the intended class, followed by detectors of the transmitted SM data vector.

A. Class Decoupling

Class decoupling techniques aim at the removal of the interference produced by the other users, and the ones presented here are based on the projection of the signal $\mathbf{y}$ on the null subspace of these interferences. All three presented strategies are based on the determination of the matrix $\mathbf{A}_n$, belonging in the left null space of $\tilde{\mathbf{H}}_n$, or:

$$\mathbf{A}_n \tilde{\mathbf{H}}_n = \mathbf{0}, \;\; \forall n \in (1, 2, ..., N) \tag{6}$$

where $\tilde{\mathbf{H}}_n$, with dimension $N_r \times (M_T - M_{T_n})$, is built excluding from $\mathbf{H}$ the columns that refer to class n, then:

$$\tilde{\mathbf{H}}_n = [\mathbf{H}_1 \;\; \ldots \;\; \mathbf{H}_{n-1} \;\; \mathbf{H}_{n+1} \;\; \ldots \;\; \mathbf{H}_N] \tag{7}$$

1) Projection in the null space of the interferences by singular value decomposition (D-SVD): This strategy uses SVD of the channel matrix $\tilde{\mathbf{H}}_n$, which contains interference components, i.e., $\tilde{\mathbf{H}}_n = \tilde{\mathbf{U}}_n \tilde{\mathbf{\Sigma}}_n \tilde{\mathbf{V}}_n^{\mathcal{H}}$, where $\tilde{\mathbf{U}}_n$ and $\tilde{\mathbf{V}}_n^{\mathcal{H}}$ are matrices comprised of singular vectors and $\tilde{\mathbf{\Sigma}}_n$ is a matrix of singular values. If r_n is the rank of $\tilde{\mathbf{H}}_n$, $r_n = rank(\tilde{\mathbf{H}}_n) \leq M_T - M_{T_n}$, SVD decomposition is expressed as:

$$\tilde{\mathbf{H}}_n = [\tilde{\mathbf{U}}_{1,n} \quad \tilde{\mathbf{U}}_{0,n}] \tilde{\mathbf{\Sigma}}_n [\tilde{\mathbf{V}}_{1,n} \quad \tilde{\mathbf{V}}_{0,n}]^{\mathcal{H}} \tag{8}$$

where $\tilde{\mathbf{U}}_{0,n}$ and $\tilde{\mathbf{V}}_{0,n}^{\mathcal{H}}$ with dimensions $N_r \times (N_r - r_n)$ and $(M_T - M_{T_n} - r_n) \times (M_T - M_{T_n})$ compose orthogonal bases of the left null space and the right null space of $\tilde{\mathbf{H}}_n$ respectively. Then, in this strategy, the matrix $\mathbf{A}_n$ is given by:

$$\mathbf{A}_n = \tilde{\mathbf{U}}_{0,n}^{\mathcal{H}}. \tag{9}$$

2) Projection in the null space of the interferences by zero-forcing filtering (D-ZF): This strategy, proposed in this paper, considers the channel inversion matrix, called zero-forcing (ZF) to perform the interference cancellation. Let $\mathbf{H}^{\dagger} = (\mathbf{H}^{\mathcal{H}}\mathbf{H})^{-1}\mathbf{H}^{\mathcal{H}}$, of dimension $M_T \times N_R$, be the ZF matrix of $\mathbf{H}$ that produces $\mathbf{H}^{\dagger}\mathbf{H} = \mathbf{I}$, that can be structured as $\mathbf{H}^{\dagger} = [(\mathbf{H}_1^z)^T \ (\mathbf{H}_2^z)^T \ \ldots \ (\mathbf{H}_N^z)^T]^T$. Then, the matrix that decouples the n-th class from the others is:

$$\mathbf{A}_n = \mathbf{H}_n^z. \tag{10}$$

3) Projection in the null space of the interferences using MMSE filtering (D-MMSE): The decoupler D-MMSE proposed in [4],[5], is obtained partitioning MMSE channel matrix of $\mathbf{H}$ given by $\mathbf{H}^{MMSE} = \mathbf{H}^{\mathcal{H}}(\mathbf{H}\mathbf{H}^{\mathcal{H}} + \sigma_n^2\mathbf{I})^{-1}$. Likewise D-ZF, $\mathbf{H}^{MMSE}$ is structured as $\mathbf{H}^{MMSE} = [(\mathbf{H}_1^m)^T \ (\mathbf{H}_2^m)^T \ \ldots \ (\mathbf{H}_N^m)^T]$. In fact, $\mathbf{H}_n^m$ is approximately in the left null space of $\tilde{\mathbf{H}}_n$. In this procedure, the bases of the vector space generated by $\mathbf{H}_n^m$ are obtained by the $\mathbf{RQ}$ decomposition of $\mathbf{H}_n^m$, this means:

$$\mathbf{H}_n^m = \mathbf{R}_n\mathbf{Q}_n, \ \ \forall n \in (1, 2, ..., N), \tag{11}$$

where $\mathbf{R}_n$ and $\mathbf{Q}_n$, have dimensions $M_{T_n} \times M_{T_n}$ and $M_{T_n} \times N_R$, are an upper triangular matrix and an orthonormal lines matrix which form the basis of the space $\mathbf{H}_n^m$, respectively. Then, the matrix that performs the separation of users of the n-th class is given by:

$$\mathbf{A}_n = \mathbf{Q}_n. \tag{12}$$

For the three strategies presented above, the decouplers act on the received signal in the BS, as given by:

$$\tilde{\mathbf{y}} = \mathbf{A}_n\mathbf{y}. \tag{13}$$

In the decoupler D-SVD, $\mathbf{A}_n$ is exactly in the left null space of the interferences. Then, can be written as:

D-SVD:

$$\tilde{\mathbf{y}}_n = \mathbf{A}_n\mathbf{H}_n\mathbf{s}_n + \mathbf{A}_n\sum_{m=1, m\neq 0}^{N}\mathbf{H}_m\mathbf{s}_m + \mathbf{A}_n\mathbf{n} \tag{14}$$

$$\tilde{\mathbf{y}}_n = \mathbf{A}_n\mathbf{H}_n\mathbf{s}_n + \mathbf{A}_n\mathbf{n} = \mathbf{U}_{0,n}^{\mathcal{H}}\mathbf{H}_n\mathbf{s}_n + \mathbf{U}_{0,n}^{\mathcal{H}}\mathbf{n}, \tag{15}$$

where $\tilde{\mathbf{y}}_n$ has dimensions $M_{T_n} \times 1$ and the noise component remains white with covariance matrix $\mathbf{K}_n = \sigma_n^2\mathbf{I}$.

For the strategy D-ZF, the application of the filter which eliminates the interferences on the class n, processes $\mathbf{y}$, as given by:

D-ZF:

$$\tilde{\mathbf{y}}_n = \mathbf{A}_n\mathbf{H}_n\mathbf{s}_n + \mathbf{A}_n\sum_{m=1, m\neq 0}^{N}\mathbf{H}_m\mathbf{s}_m + \mathbf{A}_n\mathbf{n} \tag{16}$$

$$\tilde{\mathbf{y}}_n = \mathbf{A}_n\mathbf{H}_n\mathbf{s}_n + \mathbf{A}_n\mathbf{n} = \mathbf{s}_n + \mathbf{H}_n^z\mathbf{n}, \tag{17}$$

where $\tilde{\mathbf{y}}_n$ has dimension $M_{T_n} \times 1$ and the colored noise component with covariance matrix $\mathbf{K_n} = \sigma_n^2(\mathbf{H}^{\mathcal{H}}\mathbf{H})^{-1}$.

In the strategy D-MMSE, $\mathbf{A}_n$, is approximately in the left null space of the interferences Assuming that $\mathbf{A}_n\sum_{m=1,m\neq 0}^{N}\mathbf{H}_m\mathbf{s}_m \approx \mathbf{0}$ in the expression, we obtain:

D-MMSE:

$$\tilde{\mathbf{y}}_n = \mathbf{A}_n\mathbf{H}_n\mathbf{s}_n + \mathbf{A}_n\mathbf{n} = \mathbf{Q}_n\mathbf{H}_n\mathbf{s}_n + \mathbf{Q}_n\mathbf{n}. \tag{18}$$

Besides this, $\tilde{\mathbf{y}}_n$ has dimension $M_{T_n} \times 1$ and the noise component remains white with covariance matrix $\mathbf{K}_n = \sigma_n^2\mathbf{I}$.

B. Detectors

After the separation of the intended class, the vectors transmitted by their users are retrieved using the adequate detection strategy. Here are presented SM detectors, with optimal and suboptimal performance.

1) Maximum likelihood detector in white noise (ML-W): The optimal strategy for detection of vectors of the n-th class, $\hat{\mathbf{s}}_n$, is given by the following minimization:

$$\hat{\mathbf{s}}_n = \underset{\mathbf{s}_n \in \mathcal{S}_n}{\operatorname{argmin}} \left\|\tilde{\mathbf{y}}_n - \mathbf{A}_n\mathbf{H}_n\mathbf{s}_n\right\|^2 \tag{19}$$

2) Maximum likelihood detector in colored noise (ML-C): The ML-C detector, optimal for the detection of the vectors of the n-th class can be expressed in the form::

$$\hat{\mathbf{s}}_n = \underset{\mathbf{s}_n \in \mathcal{S}_n}{\operatorname{argmin}}(\tilde{\mathbf{y}}_n - \mathbf{A}_n\mathbf{H}_n\mathbf{s}_n)^{\mathcal{H}}\mathbf{K}_{n_n}^{-1}(\tilde{\mathbf{y}}_n - \mathbf{A}_n\mathbf{H}_n\mathbf{s}_n). \tag{20}$$

The matrix $\mathbf{K}_{n_n}$ is identified as the n-th submatrix of dimension $M_{T_n} \times M_{T_n}$ on the main diagonal of $\mathbf{K}_n$ matrix defined in connection with (17).

3) Projection-Based List Detector (PBLD): This detector, proposed in [6],[7], operates in two phases: 1-sorting of the transmit antenna combinations and 2-detection of transmitted symbols, being that the number of repetitions occurred in the Phase 2 is controlled by a variable-size list. Consider that the antenna combinations used by the users of the n-th class in one transmission can be represented for the D_n-tuple $q = (p_1, p_2, \ldots, p_{D_n})$.

In this section the index of the n class, present in $\mathbf{H}_n$, $\mathbf{s}_n$ and D_n is abandoned, for simplicity of notation.

The first phase is based on the fact that the received vector tends to be closer to the space generated by the channel matrix employed in the transmission, $\mathbf{H}_{(q)}$, defined by the active antennas employed in the q-th combination of transmitting antennas, out of N_c^D possible combinations. The matrix that projects $\mathbf{y}$ in the subspace generated by $\mathbf{H}_{(q)}$ is expressed by:

$$\mathbf{W}_q = \mathbf{H}_{(q)}(\mathbf{H}_{(q)}^{\mathcal{H}}\mathbf{H}_{(q)})^{-1}\mathbf{H}_{(q)}^{\mathcal{H}}. \tag{21}$$

So, this sorter of the Phase 1 is composed by a filter bank which sort the combinations of transmitting antennas in decreasing order of the projection magnitude.

$$\{o_1 \ o_2 \ \ldots \ o_{N_c}\} = \underset{q}{\operatorname{argsort}} \left\|\mathbf{W}_q\mathbf{y}\right\|. \tag{22}$$

As a result $\|\mathbf{W}_{o_1}\mathbf{y}\| \geq \|\mathbf{W}_{o_2}\mathbf{y}\| \geq \cdots \geq \|\mathbf{W}_{o_{N_c}}\mathbf{y}\|$. The antenna combinations ordered in (22) are serially passed, starting from the D-tuple o_1 in direction to the smaller magnitude combinations, by the detector composed for the symbol to symbol discretizer applied after the ZF equalizer, $\mathbf{G}_{o_i} = \mathbf{H}^{\dagger}_{(o_i)}$, producing the candidates $\mathbf{c}_{o_i}$:

$$\mathbf{c}_{o_i} = \mathcal{D}(\mathbf{G}_{o_i}\mathbf{y}), \tag{23}$$

being $\mathcal{D}$ the function that discretizes the input vector into the symbols of the employed QAM modulation. To this candidate is determined the Euclidean distance in relation to the data vector, producing ϵ_{o_i}:

$$\epsilon_{o_i} = \|\mathbf{y} - \mathbf{H}_{o_i}\mathbf{c}_{o_i}\|\,. \tag{24}$$

This is used as the metric of quality of the candidate relative to the received data, $\mathbf{y}$,and also as the input the scheme that defines the list size λ, algorithm represented here as the function η:

$$\lambda = \eta(\epsilon_{o_i}) \tag{25}$$

Details about the operation of the control of the list size are found in [2]. The expressions (23) to (25) are sequentially repeated until that the number of processed candidates is equal or higher than the list size. Then the candidate with the smallest Euclidean distance is selected as the detected symbols vector, $\hat{\mathbf{s}}$.

4) Projection-Based List Detector with lattice reduction (PBLD-LR): The PBLD-LR detector differs from the PBLD due to the lattice reduction scheme, which reduces the loss of performance of the ZF filter in the occasions when the channel matrix is close to singular. In this scheme, the expression, (23) is modified to:

$$\mathbf{c}_{o_i} = \mathcal{D}(\mathbf{T}_{o_i}\mathcal{Q}_{LR}(\mathbf{G}_{o_i}\mathbf{y})), \tag{26}$$

where $\mathbf{G}^{LR}_{o_i}$ is the ZF filter modified for the lattice reduction, $\mathcal{Q}_{LR}$ represents the quantization in a lattice reduction domain and $\mathbf{T}_{o_i}$ the matrix that transform the channel matrix into a nearly orthogonal matrix. Details about this process are found in [7].

IV. Results

In this section the results obtained in the evaluation of performance (i.e., bit error rate BER) and computational complexity (i.e., average number of flops required per detected symbols vector) are presented for the detectors previously mentioned employing the class decoupling techniques.

The elements of the channel matrix $\mathbf{H}$ are modeled as statistically independent circularly symmetric complex Gaussian random variables, all with zero mean and unit variance. The modulation used in the transmission is QPSK.

A. 4 Users

In [6] is observed that the performance of the ML-W detector without the use of decoupling is superior in comparison to the performance ot the Projection-Based List detectors with and without lattice reduction. Meanwhile, in terms of computational complexity, is evidenced that the cost of the ML detector is much higher than the cost of other detectors.

In this example the decoupling techniques are evaluated using the scenario presented in the Figure 2. Once the decouplers are applied, the detection is done employing the previously mentioned detectors.

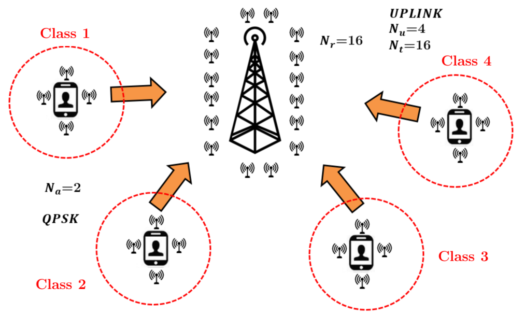

Fig. 2. Scenario of decoupling: 4 classes - 1 user per class.

As evidenced in Figure 3, the performance of the detectors that do not employ the decoupling is better than the performance of the detector with previous decoupling, that is achieved at the cost of the computational complexity significantly higher, as presented in Figure 4. The performance of the detectors using D-MMSE decoupling resulted better than those using D-SVD decoupling. As expected, the detectors using the ML-W detection get better results than those using PBLD-LR detection. One aspect to be highlighted is that the receiver with D-ZF decoupling followed by ML-C detection has the same performance that the D-SVD receiver followed by ML-W detection.

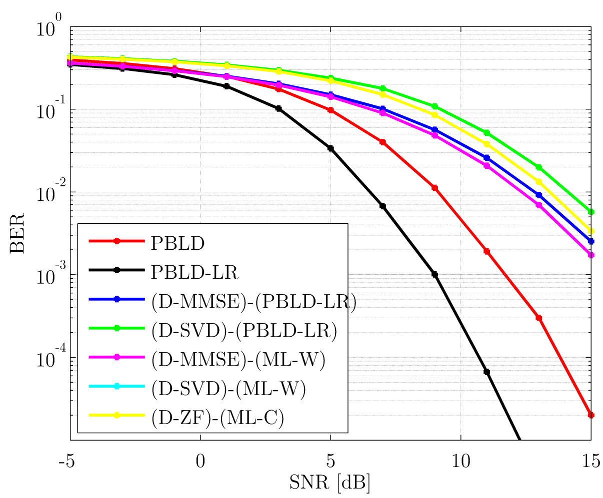

Fig. 3. Performance comparison of the decoupling techniques for 4 classes with 1 user per class ($N_{t_n} = 4$, $N_a = 2$, $N_t = N_r = 16$).

In terms of computational complexity Figure 4 shows that among the decoupling techniques the technique D-SVD requires the least number and the technique D-MMSE the greatest number of operations which is due mainly to the channel matrix inversion necessary for the decoupling.

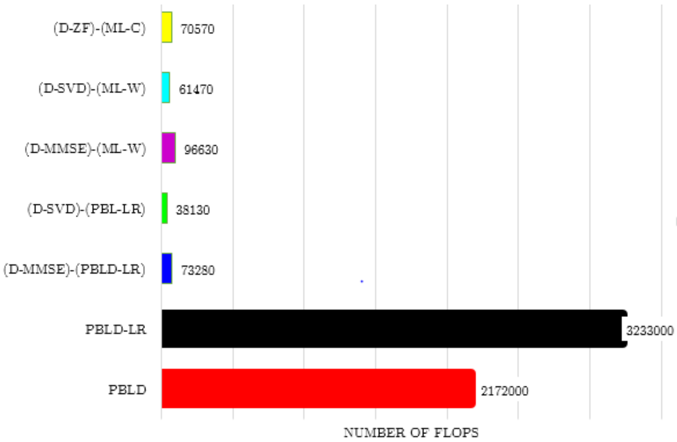

Fig. 4. Comparison in terms of computational complexity of the studied decoupling techniques for 4 classes of 1 user per class ($N_{t_n} = 4$, $N_a = 2$, $N_t = N_r = 16$).

B. 16 Users

This example considers a scenario with 16 users with the same characteristics of the users of the previous simulations. The BS uses 64 antennas for the reception. The results are presented in the Figures 5 and 6.

As in the previous scenario the performance of the detectors with D-MMSE decoupling is better than the performance of the detectors with D-SVD decoupling. The detector with ML detection achieves better performance than those that employ PBL detection.

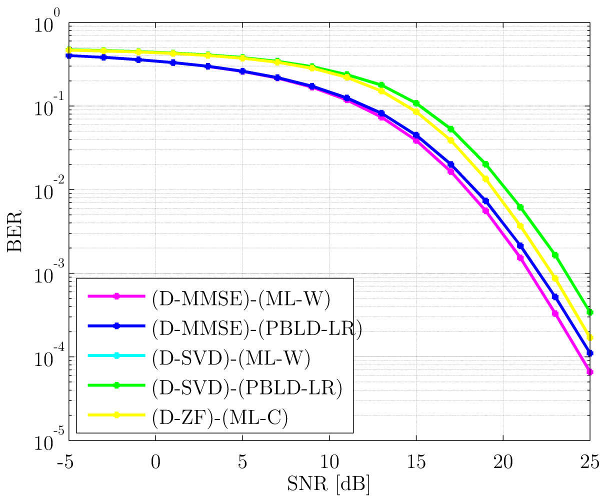

Fig. 5. Performance comparison of the decoupling techniques for 16 classes with 1 user per class ($N_{t_n} = 4$, $N_a = 2$, $N_t = N_r = 64$).

It is observed in this case that despite identical performances the ZF-ML has much lower complexity than the SVD-ML. Advantage that is accentuated in systems with higher scale and number of users.

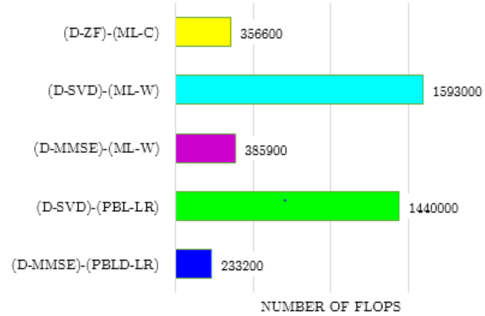

Fig. 6. Comparison in terms of computational complexity of the studied decoupling techniques for 16 classes of 1 user per class ($N_{t_n} = 4$, $N_a = 2$, $N_t = N_r = 64$).

Numeric results that consider another scenarios and include propagation and correlation effects between the antennas in the channel matrix were not included in this article due to space limitations. They can be found in [8].

V. Conclusions

The joint use of Spatial Modulation and the decoupling techniques for the signals detection is a very attractive option for the up-link in large scale MIMO systems. The extensive number of users and smart devices present in all the activities nowadays will require strategies that allow, besides of cost reduction and energy savings in the transmitters, to ensure a good detection in terms of BER and computational complexity what turns the schemes presented in this article into very promising strategies.

References

[1] M. Di Renzo, H. Haas e P.M. Grant, "*Spatial modulation for multiple-antenna wireless systems: A survey*", IEEE Commun. Mag., vol. 49, no. 12, pp. 182-191, Dec. 2011.

[2] M. Di Renzo, e H. Haas, "*On the transmit diversity for spatial modulation MIMO: Impact of spatial constellation diagram and shaping filters at the transmitter*". IEEE Trans. Veh. Technol., vol. 62, no. 6, pp. 2507-2531, Jul. 2013.

[3] J. Wang, S. Jia, e J. Song, "*Generalised spatial modulation system with multiple active transmit antennas and low complexity detection scheme*". IEEE Trans. Wireless Commun., vol. 11, no. 4, pp. 1605-1615, Apr. 2012.

[4] L. Arévalo, Rodrigo C. de Lamare, M. Haardt e R. Sampaio-Neto, "*Decoupled Signal Detection for the Uplink of Massive MIMO in Heterogeneous Networks*". EURASIP Journal on Wireless Communications and Networking, under final revision. Available at: https://arxiv.org/pdf/1611.05597

[5] L. Arévalo, "*Interference Mitigation Schemes for the Uplink of Massive in 5G Heterogeneous Cellular Networks*". Tese de Doutorado - Pontifícia Universidade Católica de Rio de Janeiro, 2016

[6] J.A. Cal-Braz e R. Sampaio-Neto, "*Projection-Based List Detection in Generalized Spatial Modulation MIMO Systems*". IEEE Communications Letters, vol. 19, no. 7, pp. 1145-1148, May. 2015.

[7] J.A. Cal-Braz, "*Detecção de sinais em sistemas multiantena com Modulação Espacial*". Tese de Doutorado - Pontifícia Universidade Católica de Rio de Janeiro, 2015.

[8] J.L. Calpa Juajinoy, "*Detecção desacoplada de sinais no enlace reverso de sistemas MU-MIMO com modulação espacial*". Dissertação de Mestrado - Pontifícia Universidade Católica de Rio de Janeiro, 2017.